

Superconductivity-Induced Anomalies in the Spin Excitation Spectra of Underdoped $\text{YBa}_2\text{Cu}_3\text{O}_{6+x}$

H.F. Fong and B. Keimer

Department of Physics, Princeton University, Princeton, NJ 08544
and Brookhaven National Laboratory, Upton, NY 11973

D.L. Milius and I.A. Aksay

Department of Chemical Engineering, Princeton University, Princeton, NJ 08544

ABSTRACT

Polarized and unpolarized neutron scattering has been used to determine the effect of superconductivity on the magnetic excitation spectra of $\text{YBa}_2\text{Cu}_3\text{O}_{6.5}$ ($T_c = 52\text{K}$) and $\text{YBa}_2\text{Cu}_3\text{O}_{6.7}$ ($T_c = 67\text{K}$). Pronounced enhancements of the spectral weight centered around 25 meV and 33 meV, respectively, are observed below T_c in both crystals, compensated predominantly by a loss of spectral weight at *higher* energies. The data provide important clues to the origin of the 40 meV magnetic resonance peak in $\text{YBa}_2\text{Cu}_3\text{O}_7$.

PACS numbers: 74.25.Jb, 74.25.Kc, 74.72.Bk

Recently a new magnetic resonance mode has been found in the superconducting state of $\text{YBa}_2\text{Cu}_3\text{O}_7$ by inelastic neutron scattering. The mode occurs at an energy of 40 meV and wavevector $\mathbf{q} = (\frac{\pi}{a}, \frac{\pi}{a})$, and disappears in the normal state [1, 2, 3]. Since this mode is a novel signature of the superconducting state in the cuprates and has not been observed in any other material, much theoretical effort has gone into its interpretation. Qualitative considerations on the basis of a BCS pairing model show that quasiparticle pair production across the superconducting energy gap can give rise to enhanced spin-flip neutron scattering below the superconducting transition, provided that the order parameter changes phase on the Fermi surface [1, 4]. More elaborate theories are required to explain the experimental features of the mode in detail, especially its sharpness in both energy and momentum. Final-state interactions between the quasiparticles [5, 6, 7, 8] as well as bandstructure anomalies [9, 10] have been suggested to account for the experimental data in the framework of a *d*-wave BCS model. Predictions derived from the interlayer pair tunneling theory of high temperature superconductivity explain most features of the neutron data without invoking such effects [11]. A more complicated order parameter with a sign change between different bands [12] and a collective mode in the particle-particle (rather than particle-hole) channel [13] have also been proposed. Clearly, more experimental information is required in order to discriminate between these divergent interpretations of the 40 meV mode. Open questions include the dependence of the energy, width, and spectral weight of the resonance peak on the doping level, and the relation between the resonance peak and the magnetic excitation spectrum in the normal state. In fully oxygenated $\text{YBa}_2\text{Cu}_3\text{O}_{6+x}$ ($x \sim 1$) the magnetic susceptibility is not strong enough to be observable by neutron scattering [1].

These issues are addressed in this Letter by systematically studying the influence of superconductivity on the magnetic excitation spectra of underdoped $\text{YBa}_2\text{Cu}_3\text{O}_7$. The doping dependence of the magnetic excitation spectrum of this system has already been characterized extensively in prior work. Briefly, the spin excitations in the antiferromagnetic regime ($x \lesssim 0.4$) are well described by spin wave theory [14, 15, 16]. For $x \gtrsim 0.4$, the magnetic response is broadened in \mathbf{q} and the spectral weight is depressed at low energies [16, 17]. We have observed similar features in our samples. However, in these second-generation experiments we have taken data with very high counting statistics and found that the onset of

superconductivity leads to a pronounced redistribution of the spectral weight. The energy of maximum spectral weight enhancement increases monotonically with the superconducting transition temperature.

The samples used for the present study were two $\text{YBa}_2\text{Cu}_3\text{O}_{6+x}$ single crystals of volumes $\sim 3 \text{ cm}^3$ and mosaic spreads 0.8° and 1.4° (full width at half maximum), respectively. The samples were oxygen-depleted in their as-grown state and were annealed in air at 640°C for different lengths of time. The average oxygen content during the anneal was monitored by thermogravimetric analysis. After the average oxygen content was adjusted by this procedure, the samples were sealed in quartz tubes and kept at 740°C for about two weeks in order to achieve a homogeneous distribution of the oxygen content. The uniform susceptibility measured on a piece cut from the first sample, shown in the inset of Fig. 2, demonstrates that the oxygen content is indeed highly homogeneous: The width of the superconducting transition ($T_c = 52\text{K}$ midpoint) is very similar to the ones reported for very high quality small crystals in this doping regime [18]. Susceptibility measurements on the second crystal revealed $T_c = 67\text{K}$ (midpoint) with a somewhat larger width. A comparison with previously reported calibrations of the lattice constants and transition temperatures [18, 19] shows that the oxygenation states of the two crystals are $x \sim 0.5 \pm 0.05$ and $x \sim 0.7 \pm 0.05$, respectively.

The neutron scattering measurements were performed at the H4M, H7 and H8 triple axis spectrometers at the High Flux Beam Reactor at the Brookhaven National Laboratory. The beam collimations were $40'-40'-80'-80'$ and the final energy was 30.5 meV for the unpolarized-beam measurements. The (002) reflection of pyrolytic graphite (PG) was used as both monochromator and analyser, and a PG filter was placed before the analyser in order to eliminate higher-order contamination of the incident beam. For the polarized-beam measurements we used Heusler alloy crystals as monochromator and analyser, beam collimations $40'-60'-80'-80'$ and 28 meV final energy. The flipping ratio was 33 (corresponding to $\sim 95\%$ beam polarization) for both horizontal and vertical guide fields at the sample. The energy resolutions were $\sim 7 \text{ meV}$ (full width at half maximum) in both cases.

Fig. 1 shows typical constant-energy scans for $\text{YBa}_2\text{Cu}_3\text{O}_{6.5}$ taken with both unpolarized and polarized beams. As previously reported [16, 17], the intensity is peaked at an in-plane wavevector of $\mathbf{q} = (\frac{1}{2}, \frac{1}{2})$. [The reciprocal space coordinates (H,K,L) are quoted in units

of the reciprocal lattice vectors $2\pi/a \sim 2\pi/b \sim 1.63\text{\AA}^{-1}$ and $2\pi/c \sim 0.53\text{\AA}^{-1}$]. At all temperatures the magnetic intensity is sinusoidally modulated as a function of the wavevector perpendicular to the CuO_2 planes, a behavior which is also characteristic of both acoustic spin waves in antiferromagnetic $\text{YBa}_2\text{Cu}_3\text{O}_{6+x}$ [14, 15, 16] and of the 40 meV resonance peak in $\text{YBa}_2\text{Cu}_3\text{O}_7$ [1, 2, 3]. Our data were taken at momentum transfers for which this intensity modulation is maximum.

Constant-energy scans with similar counting statistics were taken at a series of temperatures and fitted to Gaussians in order to extract the amplitude and width of the magnetic signal. The fitted \mathbf{q} -width does not change with temperature outside of the experimental error. By contrast, the amplitude displays a dramatic temperature dependence (Fig. 2): As previously observed [16, 17], the intensity increases gradually as T_c is approached from above. The ensuing abrupt increase by $\sim 30\%$ upon cooling through T_c is only clearly discernible due to the high counting statistics of our data and has thus far not been reported by other groups. (A sharp magnetic feature at $\hbar\omega = 27$ meV was previously observed by Tranquada *et al.* [17] at this doping level but its temperature dependence was not measured.) It provides the first direct link between superconductivity and magnetic excitations of energies comparable to the superconducting energy gap in underdoped $\text{YBa}_2\text{Cu}_3\text{O}_{6+x}$.

In principle, the observed enhancement of the neutron cross section below T_c could also arise from a superconductivity-induced phonon shift and/or linewidth change. Such effects are known to be negligible for $\mathbf{q} = 0$ phonons in underdoped $\text{YBa}_2\text{Cu}_3\text{O}_{6+x}$ [18, 20], but since the observed effect is rather subtle we used two independent methods to rule out this possibility directly at the wavevectors of interest. First, we used an unpolarized beam to monitor the phonon intensity in this energy range at high momentum transfers where lattice dynamical models [1] predict strong phonon scattering. No difference of the intensities above and below T_c was observed outside the statistical error.

Second, we used spin polarization analysis to separate the non-spin-flip (phonon) and spin-flip (magnetic) cross sections. Depending on the energy transfer, the data were taken in two scattering geometries in which momentum transfers of the forms either (H,H,L) or (3H,H,L) were accessible. Use of both configurations was necessary to avoid accidental elastic scattering which can give rise to spurious signals at certain energy transfers [1]. Typical raw

data are shown in Fig. 1b. While at energies around 30-45 meV the phonon cross section is peaked around $\mathbf{Q} = (\frac{1}{2}, \frac{1}{2})$ [1], it does not depend strongly on the in-plane momentum transfer at lower energies, as demonstrated for $\hbar\omega = 21$ meV in the figure. The spin-flip scattering is peaked at $\mathbf{Q} = (\frac{1}{2}, \frac{1}{2})$ and shows the characteristic factor-of-two polarization dependence when the neutron spin at the sample position is rotated from \mathbf{Q} -parallel (horizontal field) to \mathbf{Q} -perpendicular (vertical field) [21]. The peak in the unpolarized-beam data of Fig. 1a thus arises exclusively from magnetic scattering. The filled circles in Fig. 2 are the spin-flip peak intensity at 25 meV, corrected for the background and measured with counting statistics comparable to those of the unpolarized-beam data. The non-spin-flip scattering was measured with similar statistics and showed no change upon cooling through T_c . The excellent agreement with the unpolarized-beam data again confirms the magnetic origin of the enhanced cross section below T_c .

Fig. 3 shows the difference between spectra measured above and below T_c for both $\text{YBa}_2\text{Cu}_3\text{O}_{6.5}$ and $\text{YBa}_2\text{Cu}_3\text{O}_{6.7}$. In addition to these scans, \mathbf{Q} -scans were performed at several energies above and below T_c in order to obtain the energy and temperature dependence of the background throughout the Brillouin zone. For most of the data in the figure the background (originating mostly from single-phonon and multiphonon scattering events) was found to be temperature independent in the temperature range of interest. For the measurements taken below 18 meV in $\text{YBa}_2\text{Cu}_3\text{O}_{6.7}$ the background increases uniformly throughout the Brillouin zone by about 10% upon heating from 10K to 80K. The origin of this increase is unknown (though it could arise from multiphonon scattering), but it is unlikely to be related to magnetic excitations. However, the magnitude of the increase is too small to definitively rule out a magnetic origin by polarization analysis. The subtractions below 18 meV in the lower panel of Fig. 3 were corrected for this overall effect and thus show only differences centered at $\mathbf{Q} = (\frac{1}{2}, \frac{1}{2})$. The data were further corrected for the Bose population factor $[1 - \exp(-\hbar\omega/k_B T)]^{-1}$ in order to convert the magnetic cross section to the dynamical spin susceptibility $\chi''(\mathbf{q}, \omega)$. Following the same procedure as discussed above for $\text{YBa}_2\text{Cu}_3\text{O}_{6.5}$, we found that the 33 meV spectral weight enhancement for $\text{YBa}_2\text{Cu}_3\text{O}_{6.7}$ again sets in below T_c . The difference plots of Fig. 3 therefore directly reveal the effect of superconductivity on $\chi''(\mathbf{q}, \omega)$.

Several interesting features are apparent in the difference spectra. First, the $\text{YBa}_2\text{Cu}_3\text{O}_{6.5}$ data show that most (but not all) of the spectral weight enhancement around 25 meV is drawn from higher energies in the 30-40 meV range. In the present study we used a relatively coarse energy resolution in order to maximize the signal at high energies and were therefore confined to energies above 7 meV. Previous work with tighter resolution [16] shows that the spectral weight is suppressed at lower energies in the superconducting state, thus accounting for the remaining spectral weight. The conservation of spectral weight is expected on the basis of the total moment sum rule [22], but the fact that the resonance spectral weight is drawn from normal-state excitations of both higher and lower energy is surprising and inconsistent with the simplest picture in which the resonance is exclusively built up from states below the superconducting energy gap.

The situation is somewhat different for $\text{YBa}_2\text{Cu}_3\text{O}_{6.7}$. Below 12 meV intensity centered around $\mathbf{Q} = (\frac{1}{2}, \frac{1}{2})$ is observed *neither* in the superconducting state *nor* in the normal state immediately above T_c ($T=80\text{K}$). Because of the nonzero instrumental resolution this translates into a normal state gap of ~ 17 meV, in agreement with previous work at this doping level [16]. After adjusting for the background and the thermal population factor, the magnetic intensity in the relatively narrow energy interval between the normal state gap and the tail of the 33 meV resonance peak is not strongly affected by superconductivity outside of the experimental error. Though the evidence is weaker than for $\text{YBa}_2\text{Cu}_3\text{O}_{6.5}$, the intensity at energies above the resonance peak again appears to be suppressed in the superconducting state. Detailed theoretical work is necessary in order to relate these observations to those made with a variety of other techniques in the underdoped cuprates [23].

The data of Fig. 3 also demonstrate that the 40 meV resonance peak observed in the optimally doped compound evolves continuously with the carrier concentration. A synopsis of the data at all three doping levels is given in Fig. 4. The resonance is broadened in the deeply underdoped regime but already resolution limited for $\text{YBa}_2\text{Cu}_3\text{O}_{6.7}$. Although the data are of course too sparse to establish a functional dependence of the resonance energy on T_c or doping level, the resonance energy increases monotonically with T_c , and the presently available data are consistent with a simple proportionality. A very recent photoemission study of underdoped $\text{Bi}_2\text{Sr}_2\text{CaCu}_2\text{O}_{8+\delta}$ [24] demonstrates that the superconducting energy

gap in the single-particle density of states is independent of doping. A reconciliation of this observation with our study of the neutron peak presents a challenge to models in which both phenomena are directly related [4-12].

The data of Fig. 4 also dispel possible speculations about an essential relationship between the 40 meV resonance and a phonon of slightly higher energy (42.5 meV) and similar dynamical structure factor observed in $\text{YBa}_2\text{Cu}_3\text{O}_7$ [1]. This proximity must now be regarded as purely coincidental. Since the 42.5 meV phonon does not involve the chain oxygens, it can be used to calibrate the absolute spectral weight of the resonance at different doping levels. A preliminary normalization indicates that for both samples the resonance spectral weights are within a factor of two of $\int d(\hbar\omega) \chi''_{\text{res}}(\mathbf{q}, \omega) = 0.5$ found in $\text{YBa}_2\text{Cu}_3\text{O}_7$ [1]. Details will be given in a forthcoming full publication [25]. Note that the normal state magnetic intensity in the range $10 \text{ meV} \leq \hbar\omega \leq 40 \text{ meV}$ decreases dramatically (at least by a factor of five) in the same doping interval.

In summary, our data are consistent with previous work on underdoped $\text{YBa}_2\text{Cu}_3\text{O}_{6+x}$ in the normal state [16, 17], but additional spectral enhancements, undoubtedly analogs of the 40 meV resonance in $\text{YBa}_2\text{Cu}_3\text{O}_7$, are observed in the superconducting state. Some new and surprising aspects of the resonance are elucidated, including in particular its doping dependence and its relation to the magnetic spectrum in the normal state. Obviously, the theoretical models proposed to explain the 40 meV mode should now be tested against this more extensive data set.

Acknowledgments

We are grateful to the Brookhaven neutron scattering group for their gracious hospitality, and to P. Bourges, S. Chakravarty, V.J. Emery, A.J. Millis, H. Monien, G. Shirane, J.M. Tranquada, S.C. Zhang, and especially P.W. Anderson for helpful discussions and suggestions throughout this project. The work at Princeton University was supported by the MRSEC program of the National Science Foundation under grant No. DMR94-00362, and by the Packard and Sloan Foundations. The work at Brookhaven was supported by the US DOE under contract No. DE-AC02-76CH00016.

References

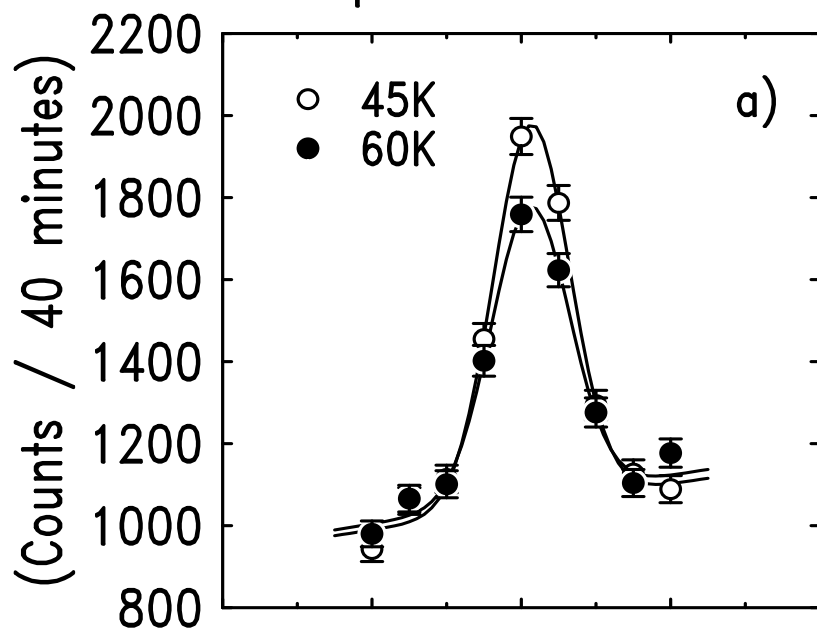
- [1] H.F. Fong, B. Keimer, P.W. Anderson, D. Reznik, F. Dogan and I.A. Aksay, Phys. Rev. Lett. **75**, 316 (1995); B. Keimer, H.F. Fong, D. Reznik, F. Dogan and I.A. Aksay, J. Phys. Chem. Solids **56**, 1927 (1995); H.F. Fong, B. Keimer, D. Reznik, D. L. Milius and I.A. Aksay, Phys. Rev. B **54**, 6708 (1996).
- [2] P. Bourges, L.P. Regnault, Y. Sidis and C. Vettier, Phys. Rev. B **53**, 876 (1996).
- [3] For earlier neutron scattering work on the 40 meV mode, see J. Rossat-Mignod *et al.*, Physica C **185-189**, 86 (1991); H.A. Mook *et al.*, Phys. Rev. Lett. **70**, 3490 (1993).
- [4] For earlier related theoretical work, see K. Maki and H. Won, Phys. Rev. Lett. **72**, 1758 (1994); P. Monthoux and D.J. Scalapino, *ibid.* **72**, 1874 (1994); H. Fukuyama, H. Kohno and T. Tanamoto, J. Low Temp. Phys. **95**, 309 (1994); F. Onufrieva and J. Rossat-Mignod, Phys. Rev. B. **52**, 7572 (1995).
- [5] D.Z. Liu, Y. Zha and K. Levin, Phys. Rev. Lett. **75**, 4130 (1995).
- [6] F. Onufrieva, Physica C **251**, 348 (1995); *ibid.* B **215**, 41 (1995).
- [7] Y. Zha, V. Barzykin and D. Pines, Phys. Rev. B **54**, 7561 (1996).
- [8] A.J. Millis and H. Monien, Report No. cond-mat/9606008.
- [9] N. Bulut and D.J. Scalapino, Phys. Rev. B **53**, 5149 (1996).
- [10] G. Blumberg, B.P. Stojkovic and M.V. Klein, Phys. Rev. B **52**, 15741 (1995).
- [11] L. Yin, S. Chakravarty and P.W. Anderson, Report No. cond-mat/9606139; P.W. Anderson (unpublished).
- [12] I.I. Mazin and V.M. Yakovenko, Phys. Rev. Lett. **75**, 4134 (1995).
- [13] E. Demler and S.C. Zhang, Phys. Rev. Lett. **75**, 4126 (1995).

- [14] J.M. Tranquada, G. Shirane, B. Keimer, M. Sato and S. Shamoto, Phys. Rev. B **40**, 4503 (1989); S. Shamoto, M. Sato, J.M. Tranquada, B.J. Sternlieb and G. Shirane, Phys. Rev. B **48**, 13817 (1993).
- [15] D. Reznik, P. Bourges, H.F. Fong, L.P. Regnault, J. Bossy, C. Vettier, D.L. Milius, I.A. Aksay and B. Keimer, Phys. Rev. B **53**, R14741 (1996); S.M. Hayden *et al.*, *ibid.* **54**, R6905 (1996).
- [16] J. Rossat-Mignod, L.P. Regnault, P. Bourges, P. Burlet, C. Vettier and J.Y. Henry, Physica B **192**, 109 (1993); L.P. Regnault *et al.*, *ibid.* **213&214**, 48 (1995).
- [17] J.M. Tranquada, P.M. Gehring, G. Shirane, S. Shamoto and M. Sato, Phys. Rev. B **46**, 556 (1992); B.J. Sternlieb, G. Shirane, J.M. Tranquada, M. Sato and S. Shamoto, Phys. Rev. B **47**, 5320 (1993).
- [18] E. Altendorf, X.K. Chen, J.C. Irwin, R. Liang and W.N. Hardy, Phys. Rev. B **47**, 8140 (1993).
- [19] R.J. Cava *et al.*, Physica C **156**, 523 (1988); *ibid.* **165** (1990); J.D. Jorgensen *et al.*, Phys. Rev. B **41**, 1863 (1990).
- [20] G. Friedl, C. Thomsen and M. Cardona, Phys. Rev. Lett. **65**, 915 (1990); M. Cardona, Physica C **185-189**, 65 (1991).
- [21] R.M. Moon, T.E. Riste and W. Koehler, Phys. Rev. **181**, 920 (1968).
- [22] S.W. Lovesey, *Theory of Neutron Scattering from Condensed Matter*, (Clarendon, Oxford, 1984).
- [23] For a brief recent review and further references, see N.P. Ong, Science **273**, 321 (1996).
- [24] J.M. Harris *et al.*, Report No. cond-mat/9611010.
- [25] H.F. Fong *et al.*, to be published.

Figure Captions

1. (a) Unpolarized-beam scans at $\hbar\omega = 25$ meV and (b) polarized-beam scans at $\hbar\omega = 21$ meV for $\text{YBa}_2\text{Cu}_3\text{O}_{6.5}$, with $\mathbf{Q} = (\text{H}, \text{H}, -5.4)$. In (a) the lines are fits to Gaussians as discussed in the text. In (b) the open (closed) symbols are data taken for horizontal (vertical) field at the sample position. The upper profile in (b) shows magnetic scattering in the spin-flip (SF) channel, while the lower profile is phonon scattering in the non-spin-flip (NSF) channel. The curves are guides-to-the-eye.
2. The open circles are the amplitudes of the magnetic cross section at $\hbar\omega = 25\text{meV}$, extracted from Gaussian fits to unpolarized-beam constant-energy scans. The closed circles are the spin-flip peak intensities measured at $\mathbf{Q} = (\frac{3}{2}, \frac{1}{2}, -1.7)$ with a polarized beam, corrected for the background and scaled to the unpolarized-beam data. The inset shows the field-cooled DC susceptibility at $H=10\text{G}$ measured by SQUID magnetometry on a small piece cut from the inside (not the surface) of the sample. Because of demagnetization effects the Meissner fraction was nominally $> 100\%$. The data were therefore normalized to the maximum susceptibility.
3. Difference between the low temperature ($< T_c$) and high temperature ($\gtrsim T_c$) magnetic susceptibility at $\mathbf{Q} = (\frac{1}{2}, \frac{1}{2}, -5.4)$. The susceptibility was obtained by adjusting the magnetic cross section for the Bose factor and for a weakly temperature-dependent featureless background at low energies in the lower panel.
4. Energy of maximum superconductivity-induced spectral enhancement as a function of the transition temperature T_c . For $\text{YBa}_2\text{Cu}_3\text{O}_{6.7}$ and $\text{YBa}_2\text{Cu}_3\text{O}_7$ the enhancement is resolution-limited in energy, and the error bars are upper bounds on the intrinsic width of the resonance.

Unpolarized Beam



Polarized Beam

